NASA TN D-4154

NASA TN D-4154

$e.1$

STRUCTURE AND KINETICS OF DEFECTS IN SILICON

by Martin M. Sokoloski

Goddard Space Flight Center
Greenbelt, Md.

NATIONAL AERONAUTICS AND SPACE ADMINISTRATION • WASHINGTON, D. C. • NOVEMBER 1967

NASA TN D-4154

STRUCTURE AND KINETICS OF DEFECTS IN SILICON

By Martin M. Sokoloski

Goddard Space Flight Center
Greenbelt, Md.

NATIONAL AERONAUTICS AND SPACE ADMINISTRATION

ABSTRACT

This paper reviews defects in the diamond-type lattice with special
emphasis on silicon which is used as the basic material in the fabri-
cation of solar cells in space programs. The defects are classified as
first, second, and higher generation defects, according to their com-
plexity. Some of these defects include vacancies and interstitials (as
in lithium, for example) which are first generation defects capable of
migrating above certain temperatures and trapping charge carriers.
These first generation defects, because of their mobility, can form
more complicated defects, such as the Si-A and Si-E centers. The
properties of such defects have been systematically tabulated. A short
discussion is given on some simple models of the kinetics of such de-
fects. A comprehensive bibliography is given at the end of the review
which should help the uninitiated commencing research in this field.

CONTENTS

STRUCTURE AND KINETICS OF DEFECTS IN SILICON

by
Martin M. Sokoloski
Goddard Space Flight Center

REVIEW OF DEFECTS IN THE DIAMOND-TYPE LATTICE

Review of the Diamond Lattice

The space lattice of diamond consists of two interpenetrating face-centered sublattices centered at $(0, 0, 0)$ and $(1/4, 1/4, 1/4)$, respectively, as shown in Figure 1. Since the diamond structure is very inefficient in packing atoms as compared with the face-centered and body-centered lattices, it is a relatively empty structure. Each atom in the diamond structure is at the center of a tetrahedron with the nearest neighbor atoms at the vertices. Because of this, the inter-atomic forces are not only central but angular-dependent. This complicates matters when calculating the lattice vibrational spectrum (Reference 2). A modified OPW method employing a pseudopotential has been successful in calculating the band structure of elements crystallizing in the diamond structure (References 3 through 6). Carbon, silicon, and germanium are some of these elements, the latter two being elemental semiconductors. Currently, silicon is being extensively used as solar cell material in the space program. Therefore, most attention will be focused on it.
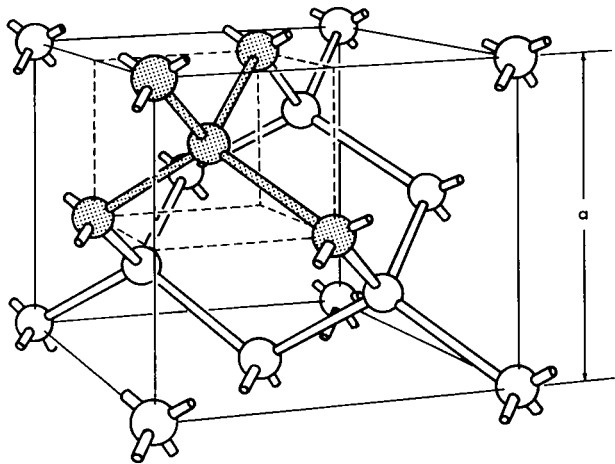

Figure 1—Crystal structure of diamond, showing the tetrahedral bond arrangement (after W. Shockley, Reference 1).

First-Generation Defects in the Diamond Lattice

First-generation defects are defined here as simple defects which are composed of not more than one defect.

1

The Lattice Vacancy

One of the simplest types of defect is the lattice vacancy—an atom missing from its lattice site shown as A in Figure 2. The electronic rebonding after the defect has relaxed is shown in Figure 3. There are three equivalent bond positions for the model; (26, 34), (23, 64) and (24, 63). A study in the temperature range of 14° to 20° K indicates an activation energy for reorientation of bonds from one equivalent configuration to another of only 0.01 to 0.02 eV at 20° K. This reorientation can also be accomplished by applying a uniaxial compressional stress along a cubic axis (Reference 7). The vacancy in silicon is capable of trapping electrons and existing in several charge states. In p-type Si, it is usually neutral, and in n-type Si a single or double negative state may exist depending upon the position of the Fermi level (see Figure 4). A positive-charge state exists but can only be seen if the sample is illuminated, since the trapping level of the positive vacancy usually lies below the acceptor impurity level. The vacancy is also capable of migrating throughout the lattice at room temperatures and below (see Figure 5). This is not surprising

A: LATTICE VACANCY
B: HOST INTERSTITIAL
C: IMPURITY INTERSTITIAL
D: "INTERSTITIAL" OXYGEN ATOM
E: DONOR IMPURITY IN SUBSTITUTIONAL POSITION
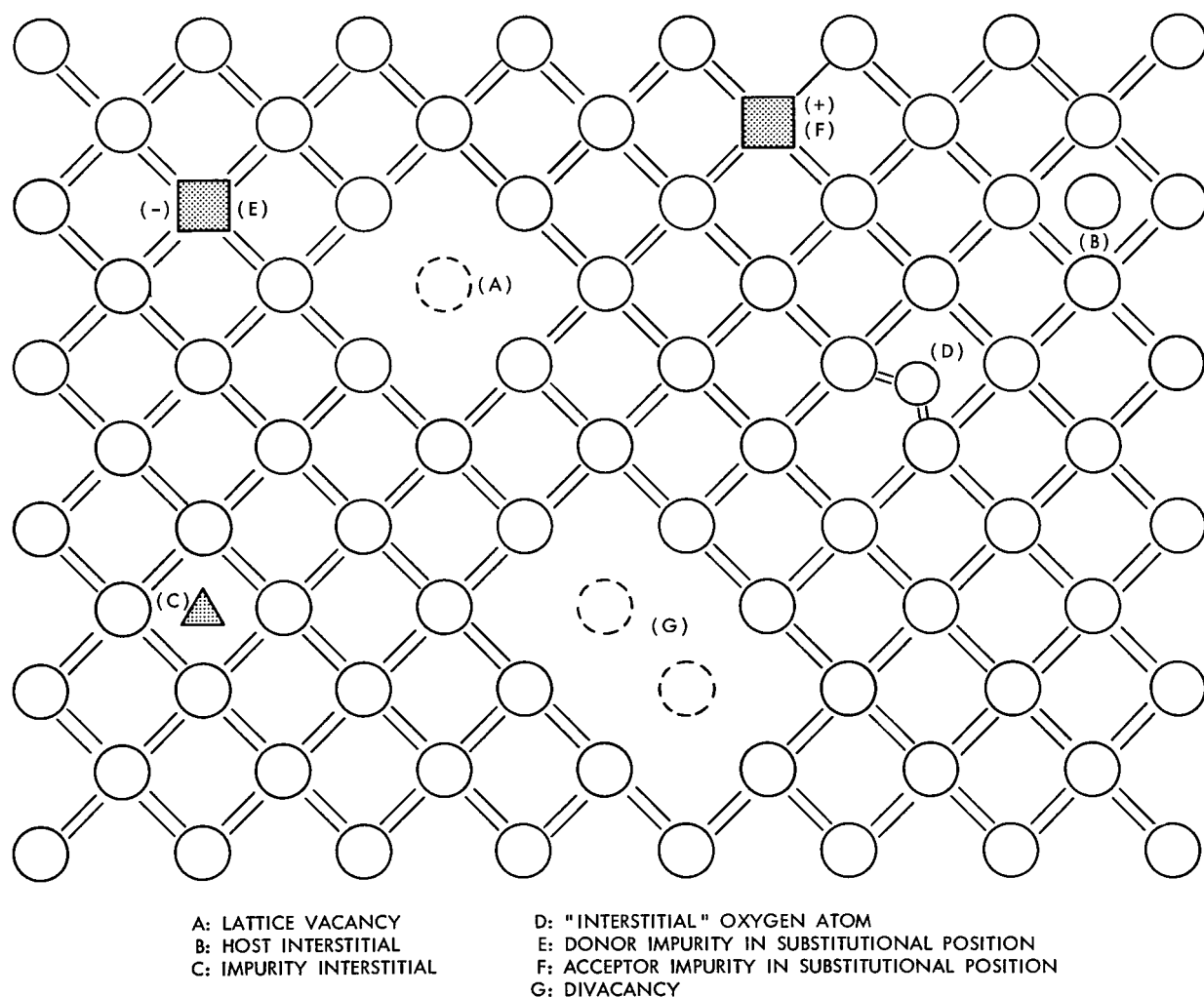F: ACCEPTOR IMPURITY IN SUBSTITUTIONAL POSITION
G: DIVACANCY

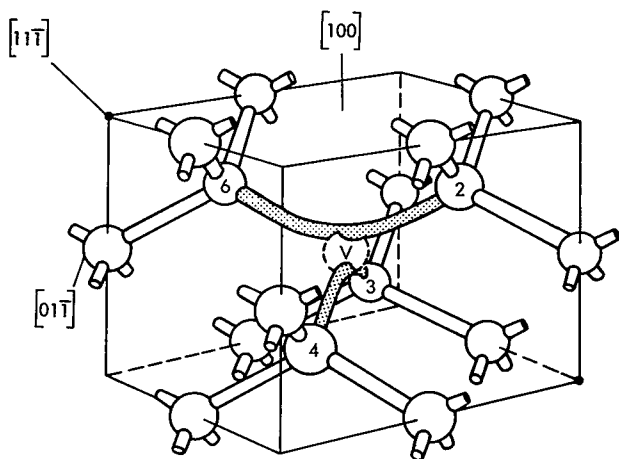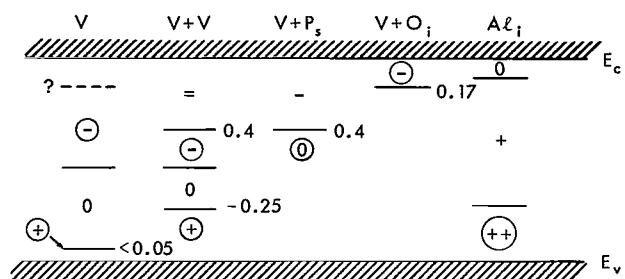Figure 2—Schematic illustration of some defects.

Figure 3—Schematic model of the vacancy in the dia-
mond lattice.

THE CIRCLED CHARGE STATES ARE THOSE OBSERVED BY EPR.

Figure 4—Electrical levels associated with some of the
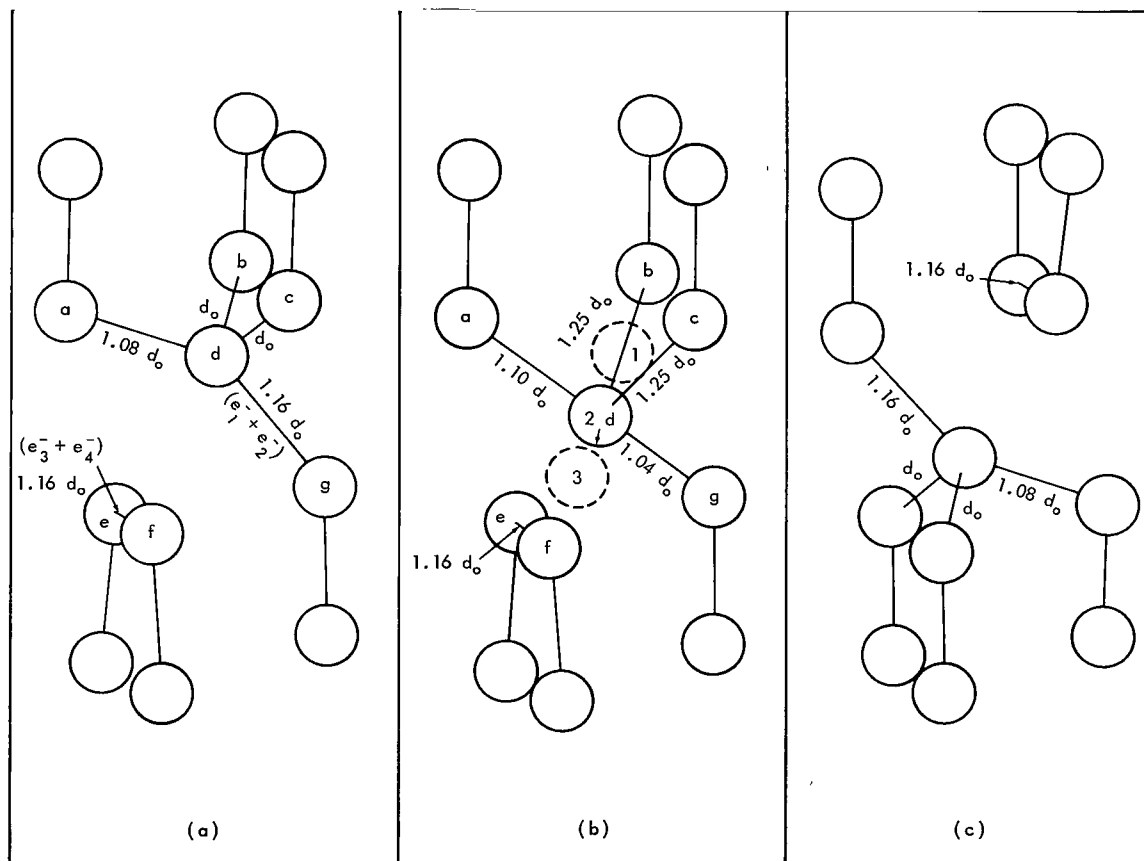defects (after G. D. Watkins, Reference 8).

(a)

(b)

(c)

Figure 5—Schematic scheme for the migration of a vacancy in the diamond
lattice (after R. A. Swalin, Reference 9).

3

since, as has been noted, the lattice is relatively open. Currently, it appears that the migration energy of the vacancy is dependent on its charge state, being 0.33 eV for a neutral vacancy and less than 0.20 eV for either negative-charge state. At this point it still is not known if the 0.20 eV energy is associated with a single or double negative state (Reference 10).

The Interstitial

Another simple type of defect is the interstitial shown as B and C in Figure 2. B represents the host atom in a nonlattice position. In the case of silicon, this would be the silicon atom. Thus far, the interstitial silicon atom has escaped detection (Reference 7). All experimental evidence indicates that the interstitial silicon is very mobile—much more than the vacancy. C represents an impurity interstitial which also can migrate throughout the lattice. Perhaps the most investigated impurity interstitials have been gold, silver, and lithium, of which lithium is of most interest. The interstitial can occupy two different symmetry sites in the lattice, the interstitial position halfway between two next neighboring atoms along a (001) lattice axis, called the tetrahedral configuration, and the position halfway between two next neighboring tetrahedral interstitial positions called the hexagonal configuration (see Figure 6). Most interstitials carry an electric charge when they enter the lattice. Lithium, copper, silver, and gold do so in silicon (References 12 through 16). However, the last three impurities can also exist as substitutional defects, and their diffusion is by the "dissociative mechanism" (Reference 17). These elements can dissolve in Si or Ge in two states, interstitially and substitutionally. To diffuse substitutionally, the host crystal must have a supply of vacancies available. Therefore, this facet of diffusion will depend strongly on the dislocation density in the crystal. The experimental values for the migration energy of Li in Si and Ge are 0.66 and 0.51 eV, respectively (Reference 18).

It is also known in radiation damage studies that interstitial Si atoms can replace dopant atoms, the dopant atoms becoming interstitials. For instance, an EPR spectrum arising from Al has been observed in aluminum-doped Si (p-type) irradiated at 4° K. There is evidence that other

(a)

○ ATOMS ABOVE PLANE OF PAPER BY 0.072 a_0

◉ ATOMS BELOW PLANE OF PAPER BY 0.072 a_0

a_0 = UNIT CELL EDGE

⊢————————⊣
a_0

(b)

(a) TETRAHEDRAL SITE – NEAREST NEIGHBOR AT 0.433 a_0 ; NEXT NEAREST NEIGHBOR AT 0.500 a_0.

(b) HEXAGONAL SITE – NEAREST NEIGHBORS AT 0.415 a_0 ; NEXT NEAREST NEIGHBORS AT 0.649 a_0.

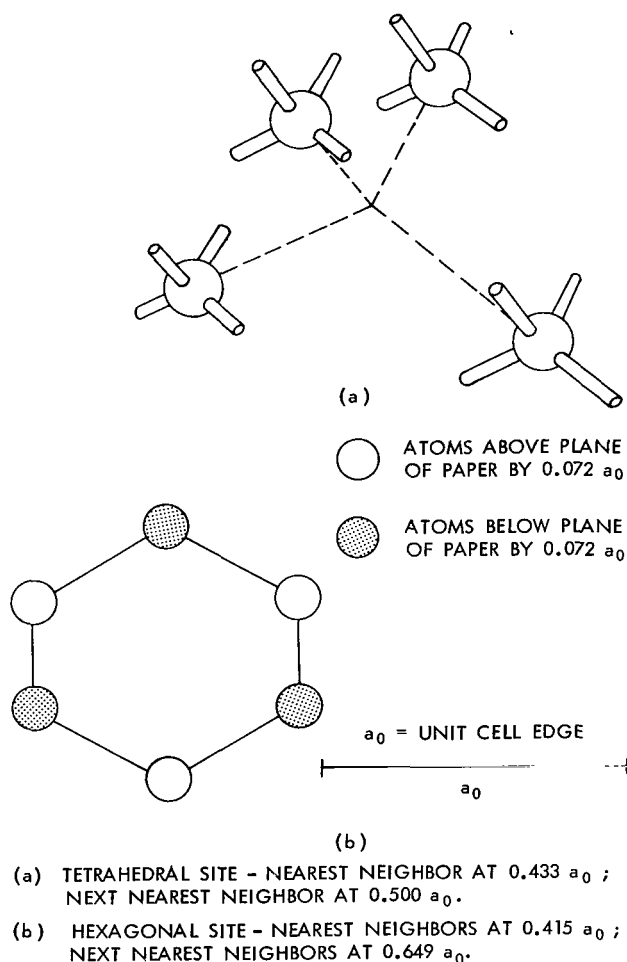THE PLANE OF THE PAPER IS NORMAL TO THE 111 DIRECTION.

Figure 6—Interstitial sites in the diamond lattice (after K. Weiser, Reference 11).

4

group III impurities behave similarly (Reference 8). The trapping levels of the interstitial Al atom are shown in Figure 4.

The Si-O-Si Configuration

This defect, which is usually seen in crystals grown in quartz crucibles, is shown as D in Figure 2. The defect will hereinafter be called the "interstitial" oxygen atom. This basic defect was first observed by its 9μ-band excitation about ν_3 shown in Figure 7. An 11.7μ-band is associated with the corresponding defect in Ge (Reference 19). There are six equivalent positions; however, Hrostowski and Alder point out that the barrier for reorientation from one

Figure 7—Model of the Si–O–Si defect or the "interstitial" oxygen atom in Si.

equivalent position to another is so small that at room temperature the Si-O-Si molecule is essentially a free rotator (Reference 20). If a uniaxial stress is applied at an elevated temperature, the <111> direction will become nonequivalent and the oxygen atom will jump to a completely new orientation. The energy required to do this is 2.561 ● 0.005 eV. This is equivalent to the energy needed for the diffusion of oxygen in the silicon lattice (References 21 and 22). The energy required for migration of the defect is so large that treating the oxygen atom as a stable defect at room temperature and below is a good approximation. This defect plays an important role in second-generation defects, discussed below.
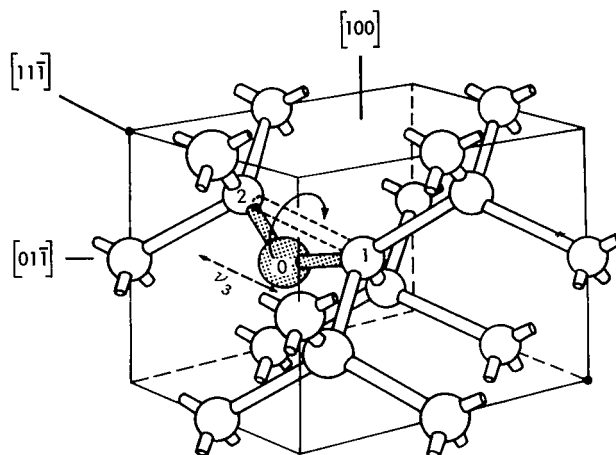
Substitutional Defects

Substitutional defects are shown as E and F in Figure 2. These defects consist of foreign atoms occupying a lattice site of the host crystal. These impurities may enter as neutral or charged substitutional defects, E being a group V donor and F being a group III acceptor. Although, when in a substitutional position, these atoms look like Si, nevertheless they are defects and should be treated as such. This will be more evident in the following section.

Second-Generation Defects

Early in the history of defects in Si and Ge, all trapping levels were thought to be due to isolated vacancies and interstitials, first-generation defects. This model soon proved to be incomplete. In reality, the vacancy not only can be a trapping and recombination center, but can migrate throughout the lattice and interact with other defects to form second-generation defects.

The Divacancy

In this defect configuration, bonding occurs between a-d and a-d' with the unpaired electron (in the solid line) between b-b', as shown in Figure 8. Besides this, there are two other equivalent

Figure 8—Model of the divacancy.
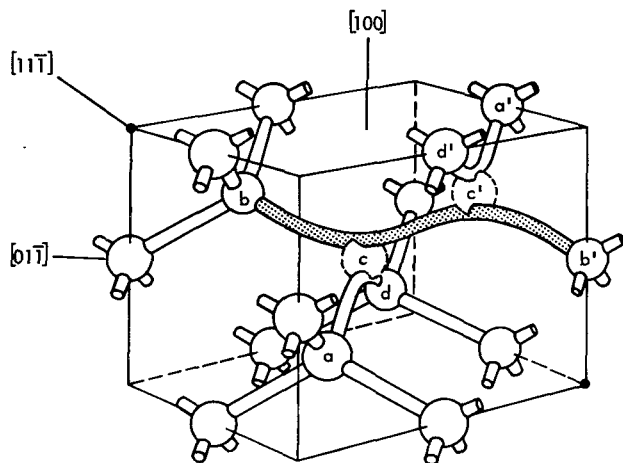
configurations: bonding a-b and a'-b' with the unpaired electron on d-d', and bonding b-d and b'-d' with the unpaired electron on a-a' (see Figure 9). By stressing the crystal uniaxially, the majority of defects can be preferentially aligned in one direction. These preferentially aligned defects can then be frozen in at a low temperature. Then by a slow isochronal anneal, the energy of reorientation of the electronic bond can be measured. In the temperature range from 40° to 110° K, line broadening is observed in the EPR spectrum of the defect (Reference 24). The energy of activation for electronic reordering is 0.06 eV. Nevertheless, another degree of freedom of the divacancy is about a line joining the vacancies. In order to change the orientation of this axis, an energy of 1.3 eV is required (Reference 24). This is actually the energy needed for the migration of such a defect. These various energies are classified in Figure 10. The trapping levels associated with the divacancy are rather complicated, as can be seen from Figure 4. The energy needed for the complete breakup of the divacancy is approximately 1.85 eV; i.e., the sum of the energy needed to separate the divacancy to the first nearest neighbor, 1.3 eV, and the corresponding energy needed to move the vacancies away from each other more than one nearest-neighbor distance, 0.65 eV (Reference 24). During low-energy electron irradiation, most of the divacancies are correlated; this is demonstrated by the anisotropy, R, of the vacancy orientation versus bombarding electron energy, where R is the ratio of the number of divacancies orientated along the beam axis to that along another, <111>, direction. For bombardment energies less than 1.0 MeV, R = 2.0 (Reference 25). At these bombardment energies, the rate of growth of divacancies is less governed by the diffusion of vacancies than at higher energies. The 1.8μ, 3.3μ and 3.9μ absorption bands have since been associated with electronic energy transitions of the divacancy (Reference 26). These bands are
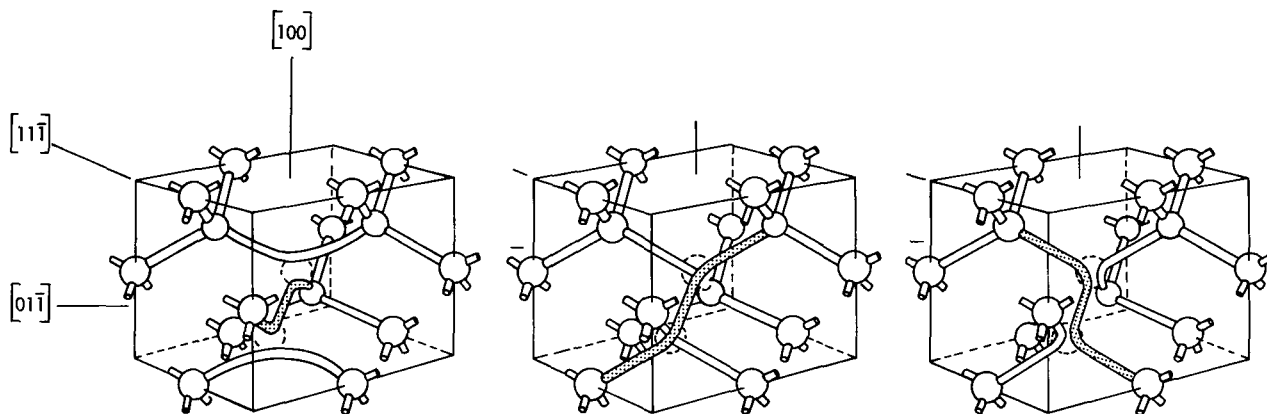

Figure 9—Three equivalent electronic orientations of the divacancy
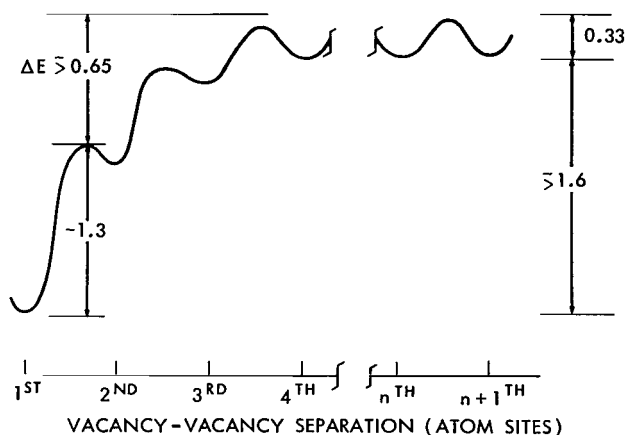(after R.P.I. progress report, Reference 23).

associated with excitation charge carriers into traps. As a result there is no photoconductivity connected with these absorption bands.

The Oxygen-Vacancy Defect in Si or the Si-A Center

In migrating throughout the lattice, the vacancy may encounter the structure in Figure 7. If so, it becomes trapped by the "interstitial" oxygen atom and forms the oxygen-vacancy complex shown in Figure 11. The configuration has an acceptor level at $E_c - 0.17$ eV. The oxygen-vacancy defect can capture an electron. After this, a hole can be captured and recombined with the electron. The defect is neutral when capturing an electron, and negatively charged before it captures a hole. The capture cross section is for electrons, $\sigma_e \simeq 10^{-16}$ cm^2, and for holes, $\sigma_h \simeq 10^{-14}$ cm^2 (Reference 27). Again, there are six equivalent configurations for the oxygen-vacancy defect, the energy required for electronic reorientation being 0.20 ± 0.03 eV (Reference 28). Also, the defect itself can change positions corresponding to an applied stress. The energy required corresponds to 0.38 ± 0.04 eV for a neutral oxygen-vacancy defect (Reference 28). This energy is the thermal-activated switching of the oxygen atom from one pair of silicon atoms to another. The oxygen-vacancy defect gives rise to an impurity vibrational band at 12μ (Reference 29). The trapping level at $E_c - 0.17$ eV and the 12μ band disappear upon an isochronal anneal to 500° C, indicating an activation energy of 1.3 eV for possible breakup (Reference 30).

NEIGHBOR POSITIONS ARE SHOWN IN ORDER OF INCREASING SEPARATION; THESE ARE NOT NECESSARILY IN A STRAIGHT LINE.

Figure 10—The potential energy (in eV) of one neutral vacancy in the vicinity of another (after G. D. Watkins and J. W. Corbett, Reference 24).
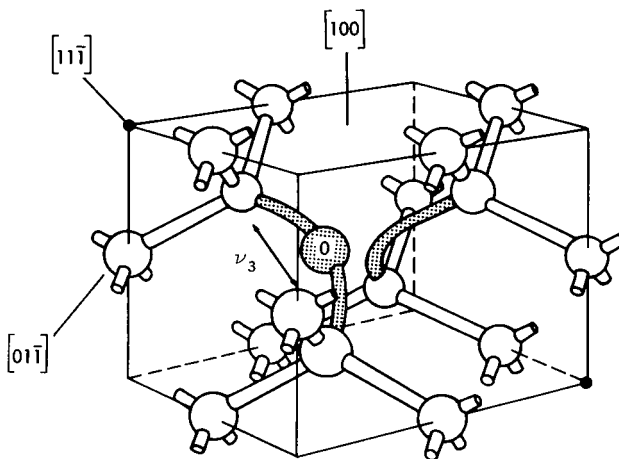
Figure 11—A model of the oxygen-vacancy complex or the Si-A center.

The Phosphorus-Vacancy Defect in Si or the Si-E Center

As in the oxygen-vacancy defect, the vacancy, if encountering a phosphorus atom in a substitutional position, can become trapped and thus form the phosphorus-vacancy defect shown in Figure 12. Again there are three equivalent electronic orientations. The energy needed to activate the hopping of an unpaired electron from one configuration to another is 0.06 eV (Reference 31).

7

The energy required to change the direction of the phosphorus-vacancy axis by rearranging atoms through a compression along a 110 axis at high temperature is 0.93 ± 0.05 eV (Reference 31). This reorientation amounts to diffusion of the phosphorus-vacancy pair through the lattice. It is not known if the phosphorus-vacancy defect breaks up or diffuses as an entity to traps, as pointed out by Watkins. Some annealing experiments give 0.93 eV as the activation energy for annealing, suggesting diffusion to traps (Reference 27). An argument by Watkins and Corbett gives the energy of annealing as 1.18 eV. This information is condensed in Figure 13. This defect has a deep acceptor level at E_c - 0.40 eV. So far, there is no evidence of an associated lattice vibrational band. The defect has a hole capture cross section of 1.1×10^{-13} cm^2 (References 27 and 32).
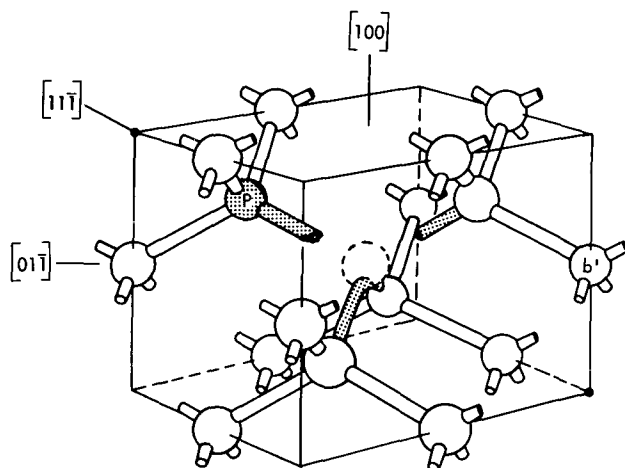

Figure 12—A model of the phosphorus-vacancy complex or the Si-E center.

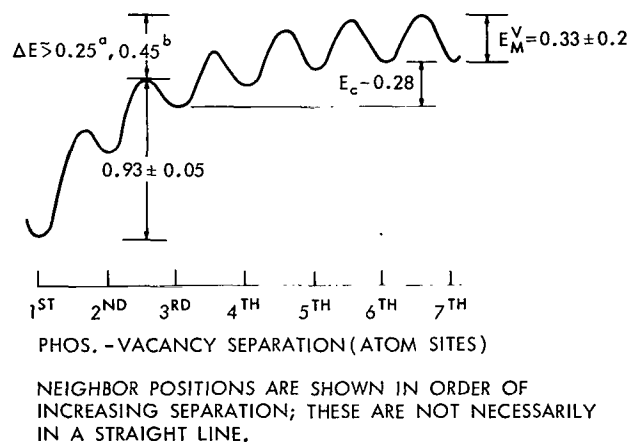NEIGHBOR POSITIONS ARE SHOWN IN ORDER OF INCREASING SEPARATION; THESE ARE NOT NECESSARILY IN A STRAIGHT LINE.

Figure 13—The potential energy (in eV) of a vacancy in the vicinity of a substitutional phosphorus atom (after J. W. Corbett, G. D. Watkins, R. M. Chrenko, and R. S. McDonald, Reference 29).

Other Impurity-Vacancy Defects

The silicon crystal can also be doped with other group V elements besides phosphorus. Studies on silicon doped with As, Sb, and Bi indicate that each of these impurities can form an impurity-vacancy defect in Si with trapping levels around E_c - 0.40 eV and configurations similar to the phosphorus-vacancy complex. An empirical formula has been obtained for the activation energy of annealing these centers:

$$E_a = 3.6r - 3.0 \text{ eV},$$

where E_a is the activation energy for annealing the defect, r is the tetrahedral covalent radius of the impurity atom of group V in A° (Reference 33).

The A_s-vacancy defect has a hole capture cross section of 4×10^{-14} cm^2 (Reference 27).

There is also a possibility of group III atoms contributing to impurity-vacancy defects. For instance, in Al-doped vacuum floating-zone Si, an EPR spectrum is observed to grow; this is

associated with the disappearance of the free vacancy spectrum along with the A1 (Reference 27) hyperfine interaction (Reference 8). No trapping levels have so far been associated with this A1-vacancy defect.

Ion-Pairing

Perhaps the most extensively studied interstitial in the Si lattice is the Li^+ ion which enters the lattice as a donor (References 12 and 34). In p-type Si, the Li^+ interstitials are known to interact with the p-type dopant atoms to form relatively immobile Li-dopant ion pairs (References 35, 36, and 37). It is also known that the Li^+ interstitial will interact with the "interstitial" oxygen atom to form $(Li-O)^+$ defects. The dissociation or annealing energy of such complexes is obtained from the ratio of the effective drift mobility of Li in samples with oxygen concentrations up to 1.3×10^{18} cm^{-3} to known drift mobility of free Li, and is 0.42 eV (Reference 37). The absorption peaks for Li-B pairing have been observed by W. G. Spitzer and M. Waldner and are reproduced in Table 1 (Reference 38). Some of their conclusions are:

1. The modes at 564 or 584 and at 655 or 681 cm^{-1} do not involve much Li motion.

2. The position of these modes does depend upon a change of the local environment around the boron atom due to the Li ion, paired with the boron.

3. The force constant between the paired Li and B is not great enough to cause a characteristic Li-B vibration.

Table 1

Number of Dominant Frequency Absorption Bands Upon "Annealing" the Oxygen-Vacancy Defect in Li.

Isotopic pair/cm^{-1}	11_B & 7_{Li}	10_B & 7_{Li}	11_B & 6_{Li}	10_B & 6_{Li}
Low-frequency peak	522	522	534	534
Central-frequency peak	564	584	564	584
High-frequency peak	655	681	657	683
Peak due to unpaired boron	620	644		

Higher-Generation Defects

It was mentioned that the phosphorus-vacancy defect could migrate at an energy and become trapped, possibly forming another defect. Also, the migration energy of the oxygen-vacancy complex is such that this entity could migrate and form higher-order defects. Obviously the classification of these defects along with other more complicated defects can get out of hand. Therefore, the classification of defect conglomerations composed of three or more first-generation defects will be called higher-generation defects.

Upon monitoring the decay of the impurity vibrational band of the oxygen-vacancy defect in Si at 829 cm^{-1} (12μ), Corbett, Watkins, and McDonald noticed the appearance of other new bands at 887 cm^{-1} (11.215μ), 904 cm^{-1} (11.004μ), 968 cm^{-1} (10.276μ), and 1000 cm^{-1} (9.948μ). The rise of the 887 cm^{-1} line is interpreted as the diffusion of an oxygen-vacancy defect to an "interstitial" oxygen site as shown in (a) of Figure 14, and is hereinafter called the CWM I defect. The remaining three bands would be caused by the addition of another "interstitial" oxygen atom to CWM I. This configuration shown as (b) in Figure 14 will be called the CWM 2 defect (Reference 39). As stated in Reference 39, these models are highly speculative. It is not known if either CWM 1 or 2 acts as trapping or recombination centers. Since the experiment of CWM, other spectra shown in Table 2 have been seen upon annealing the oxygen-vacancy defect. Four of the lines have been seen and correlated by two or more investigators, including the 12μ, 11.3μ, 11.0μ, and 9.0μ lines (References 40, 41 and 42). (The slight differences between the values of Corbett, et al. and those of the other three investigators are due to a different measuring temperature.) This clearly demonstrates that the oxygen-vacancy defect need not decompose into its first-generation defects, but may form higher-generation defects. This may also be the case with other second-generation defects upon annealing.
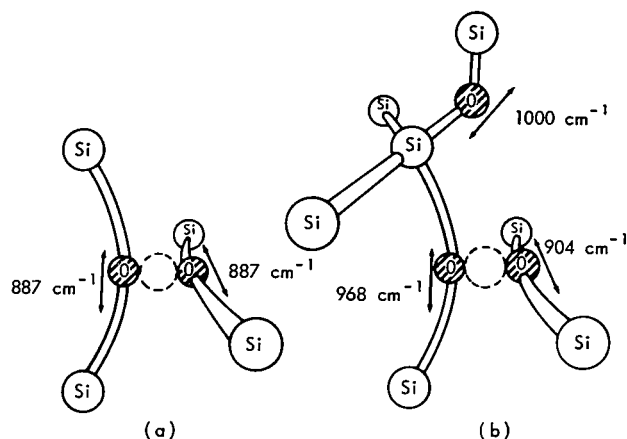

Figure 14—Tentative models for (a) the 887 cm^{-1} ir band and (b) 904-, 968-, and 1000-cm^{-1} bands (after E. M. Pell, Reference 35).

Table 2

Associated Spectra Due to Li and Boron Pairing.

Investigator	Dominant Band in (Wave Numbers, Cm^{-1}) in Microns											
	Cm^{-1}	(488)	(834)	(865)	(894)	(904)	(922)	(932)	(936)	(968)	(984)	(1000)	(1106)
	μ	20.5	12	11.6	11.3	11	10.8	10.74	10.69	10.28	10.17	9.95	9
R. E. Whan (Reference 40)			X	X	X		X	X	X				X
J. C. Corelli, et al. (Reference 41)			X	X									X
J. W. Corbett, et al. (Reference 39)			X		X	X				X	X	X	X
H. Y. Fan (Reference 42)		X	X										X

The Silicon K Center

This defect is one of the predominant paramagnetic defects introduced into p-type silicon. This center requires oxygen and acts as a hole trap at $E_v + 0.30$ eV. Its charge state can also change, depending on the position of the Fermi level (Reference 44). A speculative model proposed from EPR measurements by a group at RCA is shown in Figure 15 (Reference 45). Two oxygen-vacancy complexes can randomly migrate throughout the crystal and, upon a chance meeting, form such a defect configuration. The probability of this event occurring is more likely than two vacancies being trapped by a Si-O-O-Si molecule. Unfortunately, no impurity lattice vibrational mode has yet been seen or measured corresponding to this center. It would be interesting to see if any of the absorption peaks of the K-center correspond to any of those for CWM 1 or 2.
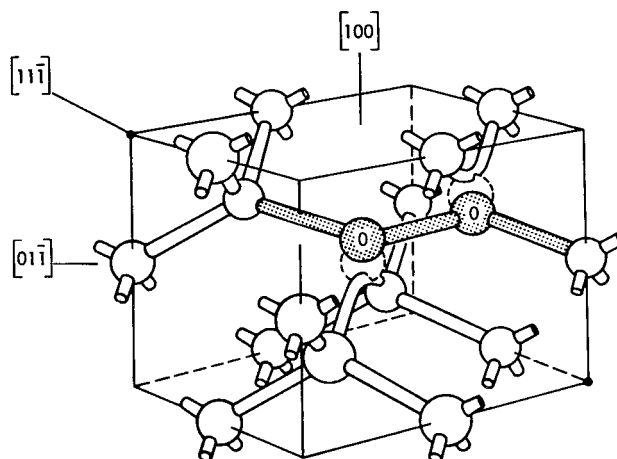

Figure 15—RCA tentative model for the K-center.

Conclusions

All the kinetic properties of the various defects are given in Table 3. The contributors to the various experimental values which are unreferenced in the table can be found in the main text, and

Table 3
Defects in Li and Their Properties.

Defect	Energy Parameters in eV			Associated Lattice Absorption Band (μ)	Impurity Electronic Energy States
	Electronic Reorientation	Migration Energy	Annealing Energy		
Vacancy	0.01 - 0.02	0.30 (neutral) .20 (charged)[a]	-	-	three charged states see Figure 4
Silicon interstitial	-	0.02	-	-	?
"Interstitial" oxygen	0.02	2.56	-	9μ	none
Divacancy	0.06	1.3	1.85[b]	?	double neg. single neg. see neutral Figure 4 single pos.
Oxygen-vacancy	0.20 0.03	0.38[c]	1.3	12μ	single neg at E_c - 0.17 eV
Phosphorus-vacancy	0.06[d]	0.93 0.05	1.18[e] 1.38[f]	?	single neg at E_c - 0.40 eV
Li^{+}	-	0.655	-	-	acts as a donor
(Li - O)[+]	-	-	0.42	?	acts as a donor
Li^{+} + B[-]	-	Continued:	-	see text	-
CWM 1	-	-	-	11.215 (887 cm^{-1})	?
CWM 2	-	-	-	9.948 (1000 cm^{-1}) 10.276 (968 cm^{-1}) 11.004 (904 cm^{-1})	?
K-center	-	-			E_v + 0.3 eV, (hole trap)

(a) May be a single or double negative charge state.
(b) This is presumably for a neutral divacancy. This energy probably depends on the charge state of the defect.
(c) Energy required to break an Si-O bond for neutral Si-A defect
(d) The energy required for the hopping of one unpaired electron between the three equivalent directions.
(e) From EPR measurements.
(f) From electrical measurements.

need not be repeated in the table. This list of defects is by no means exhaustive. Future developments will add to the list and disagreements will persist, i.e.

1. Quenching experiments in p-type Si report an energy of migration of the interstitial of 0.31 eV (Reference 46).

2. No theoretical calculations substantiate any values for the experimental values of the energy of migration of either the vacancy or interstitial (References 47 and 40).

The vacancy is the defect which is responsible for most of the damage in the silicon lattice. Without it, most second- and higher-generation defects would not exist. Therefore, the importance of establishing a well based theoretical calculation which agrees with the experimental value of the migration energy of the vacancy cannot be overstated.

KINETICS OF DEFECT PRODUCTION AND MIGRATION

The simple laws of mass action can be used with some success in following the various interactions of defects in solids. In this simple notation, the creation of an impurity-vacancy defect by a source of radiation, ϕ, can be schematically written in the form of three reactions:

$$\phi \xrightarrow{\text{K}_0} V + i , \tag{1}$$

$$V + i \xrightarrow{\text{K}_1} \text{annihilation} , \tag{2}$$

$$V + I \xrightleftharpoons{\text{K}_2} C , \tag{3}$$

where

V is the free-vacancy concentration,
i is the free-interstitial concentration,
I is the free-impurity concentration,
C is the 2nd-generation defect concentration.

These concentrations are measured in atomic fractions. The side conditions are:

$$i = V - C ,$$

$$I = I_0 - C ,$$

where I_0 is the impurity concentration at time $t = t_0$. The reaction rates, K_i, are defined as follows:

$$K_i = \gamma_i \, \nu_i \, \exp\left(-E_i/kT\right) ,$$

where

γ_i is the coordination number,

ν_i is the frequency factor,

E_i is the energy associated with the particular reaction,

k is Boltzmann's constant,

T is the temperature.

This model assumes, of course, that the interstitials are captured at sinks with rates much less than the K_i's defined. Actually, the reaction rate for trapping of interstitials by sinks such as the surface is so small compared to the other reaction rates that it can be neglected. Reaction 1 is just the creation of first-order defects (Frenkel pairs) through some source term ϕ, with an efficiency factor K_0. Reaction 2 is the annihilation of these first-generation defects by chance meeting. Finally, reaction 3 is the trapping of vacancies by impurities to form second-generation defects, in this case impurity-vacancy defects. The differential equations become:

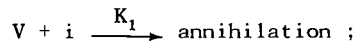$$\frac{dV}{dt} = -K_2 I_0 V + K_3 C - K_1 V^2 + \left(K_2 - K_1\right) VC + K_0 \phi \tag{4}$$

$$\frac{dC}{dt} = K_2 I_0 V - K_3 C - K_2 VC . \tag{5}$$

These have been solved by computer program; asymptotic analytic solutions have been obtained for long times, low temperatures, and $K_3 \approx 0$.

Reaction 3 is shown as being reversible. However, in the discussion of higher-generation defects, it is shown that the production of such defects is not only possible but likely. In annealing studies where the source term is now zero, the kinetic scheme would have to be replaced by more complicated reactions. For example:

$$C \xrightarrow{K_3} V + I , \tag{6}$$

$$C + C \xrightarrow{K_4} C_2 , \tag{7}$$

$$C + V \xrightarrow{K_5} C_3 , \tag{8}$$

and, if any interstitials are still present,

$$V + i \xrightarrow{K_1} \text{annihilation} ;$$

otherwise $K_i = 0$. The differential equations would then be

$$\frac{dC}{dt} = -K_3 C - K_4 C^2 - K_5 CV , \tag{9}$$

13

$$\frac{dC_2}{dt} = K_4C^2 , \tag{10}$$

$$\frac{dC_3}{dt} = K_5CV , \tag{11}$$

$$\frac{dV}{dt} = K_3C - K_1V_i . \tag{12}$$

In the case of the oxygen-vacancy defect in Si, reaction 7 would possibly be the production of the RCA K-center. At the present, higher-generation defects associated with the impurity oxygen atom have only been seen, but these reactions should not be ruled out for other impurities, such as the phosphorus-vacancy defect. In the case of measuring some electrical parameter, the "annealing" of the sample is usually seen as the trapping or expulsion of trapped carriers. If, upon "annealing", the resultant higher-generation defects were capable of trapping additional carriers, then there would be "reverse annealing". This can best be seen by counting charges:

$$V + I \xrightarrow{K_2} C - Me^{\pm}$$

$$C + \xrightarrow{K} C_2 \cdot^- (M + \ell) e^{\pm} .$$
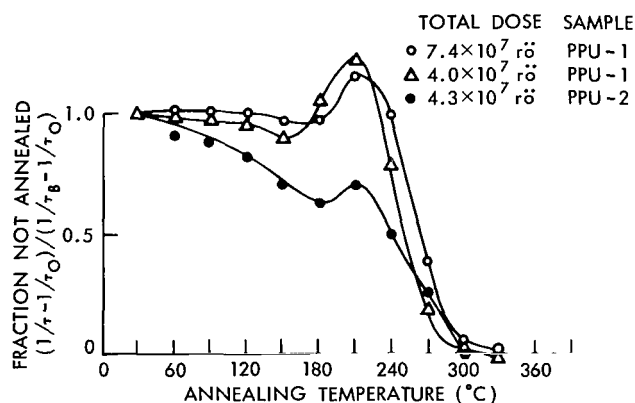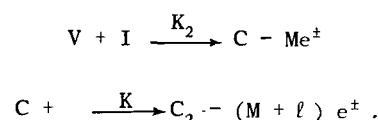

Figure 16—Reverse annealing of electrical parameters in Si (after T. Nakano, K. Nakasima, and Y. Inuishi, Reference 48).

The result of the anneal will be the additional loss of 1 charges. However, an isochronal measurement of the intensity of the defect absorption bands together with photoconductivity will only show forward annealing of C and production of C_2. An example of reverse annealing in the experiments of T. Nakano, et al. is shown in Figure 16. These curves are not atypical.

REFERENCES

1. Shockley, W., "Electrons and Holes in Semiconductors," New York, Van Nostrand, 1950.

2. Smith, Helen M. J., "The Theory of the Vibrations and the Raman Spectrum of the Diamond Lattice," *Phil. Trans. Roy. Soc.* (London), (A241): 105-145, 1948.

3. Herman, F., "Electronic Structure of the Diamond Crystal," *Phys. Rev.* 88: 1210-1211, 1952.

4. Phillips, J. C., "Band Structure of Silicon, Germanium and Related Semiconductors," *Phys. Rev.*, 125: 1931-1936, 1962.

5. Kleinman, L., and Phillips, J. C., "Crystal Potential and Energy Bands of Semiconductors. 1. Self Consistent Calculations for Diamond," *Phys. Rev.* 116: 880-884, 1959.

6. Benneman, K. H., "Covalent Bonding in Diamond," *Phys. Rev.* 139: (A482-A488), 1965.

7. Watkins, G. D., "An Electron Paramagnetic Resonance (E.P.R.) Study of the Lattice Vacancy in Silicon," *J. Phys. Soc. Japan,* 18: Suppl II: 22-27, 1963.

8. Watkins, G. D., "Radiation Damage in Semiconductors," 7th International Conference on Physics of Semiconductors, Paris, 1964, p. 259.

9. Swalin, R. A., "Theoretical Calculations of the Enthalpies and Entropies of Diffusion and Vacancy Formation in Semiconductors," *J. Phys. Chem. Solids,* 18: 290-296, 1961.

10. Gregory, B. L., "Injection Stimulated Vacancy Reordering in p-Type Silicon at 76 K," *J. Appl. Phys.* 36: 3765-3769, 1965.

11. Weiser, K., *Phys. Rev.,* 126: 1427, 1962.

12. Fuller, C. S., and Severiens, J. C., "Mobility of Impurity Ions in Germanium and Silicon," *Phys. Rev.* 96: 21-24, 1954.

13. Gallagher, C. J., "Electrolysis of Copper in Solid Silicon," *J. Phys. Chem. Solids,* 3: 82-86, 1957.

14. Kosenko, V. E., "Diffusion and Solubility of Cadmium in Germanium," *Fiz. Tverdogo Tela,* 1. 1622-1626, 1959.

15. Boltaks, B. I., and Shih-yin, H., "Diffusion, Solubility, and the Effect of Silver Impurities on the Electrical Properties of Silicon," *Fiz. Tverdogo Tela,* 2: 2677-2684, 1960.

16. Boltaks, B. I., Kulikov, G. S., and Malkovich, R. Sh., "The Effect of Gold on the Electrical Properties of Silicon," *Fiz. Tverdogo Tela,* 2: 181-191, 1960.

17. Frank, F. C., and Turnbull, D., "Mechanism of Diffusion of Copper in Germanium," *Phys. Rev.* 104: 617-618, 1956.

18. Reiss, H., and Fuller, C. S., "Diffusion Processes in Germanium and Silicon," Chapter VI *in:* Hannay, N. B., "Semiconductors," New York, Reinhold Corp., 1959.

19. Hrostowski and Kaiser, "Infrared Absorption of Oxygen in Silicon," *Phys. Rev.* 107: 966-972, 1957.

20. Hrowstowski and Alder, "Evidence for Internal Rotation in the Fine Structure of the Infrared Absorption of Oxygen in Silicon," *J. Chem. Phys.* 33: 980-990, 1960.

21. Corbett, J. W., McDonald, R. S., and Watkins, G. D., "The Configuration and Diffusion of Isolated Oxygen in Silicon and Germanium," *J. Phys. Chem. Solids,* 25(8): 873-879, 1964.

22. Southgate, P. D., "Internal Friction in Germanium and Silicon I: Electron and Impurity Relaxation," *Proc. Phys. Soc. London,* 76: 385-397, 1960.

23. R. P. I. progress report, NASA grant NsG-290 period March 1965-September 1965.

24. Watkins, G. D., and Corbett, J. W., "Defects in Irradiated Silicon: Electron Paramagnetic Resonance of Divacancy," *Phys. Rev.* 138: (A543-A555), 1965.

25. Becker, Milton, "The Infrared Optical Properties of Germanium and Silicon, 87 p. PhD. Thesis, Purdue University, 1951.

26. Cheng, L. J., PhD. thesis, R. P. I.

27. Hirata, M., Hirata, M., and Saito, H., "Recombination Centers in Gamma-Irradiated Silicon," *J. Appl. Phys.* 37: 1867-1872, 1966.

28. Watkins, G. D., and Corbett, J. W., "Defects in Irradiated Silicon. 1. Electron Spin Resonance of the Si-A Center," *Phys. Rev.* 121: 1001-1014, 1961.

29. Corbett, J. W., Watkins, G. D., Chrenko, R. M., and McDonald, R. S., "Defects in Irradiated Silicon. II. Infrared Absorption of Si-A Center," *Phys. Rev.* 121: 1015-1022, 1961.

30. Bemski, G., and Augustyniak, W. M., "Annealing of Electron Bombardment Damage in Silicon Crystal," *Phys. Rev.* 108: 645-648, 1957.

31. Watkins, G. D., and Corbett, J. W., "Defects in Irradiated Silicon: Electron Paramagnetic Resonance and Electro-Nuclear Double Resonance of the Si-E Center," *Phys. Rev.* 134: (A1359-1377), 1964.

32. Saito, H., Hirata, M., and Horiuchi, T., "Annealing of Radiation Defects in Silicon Single Crystals," *J. Phys. Soc. Japan,* 18, Suppl III: 246-250, 1963.

33. Hirata, M., Hirata, M., and Saito, H., "Annealing of E Center in Irradiated Silicon," *Japan J. Appl. Phys.* 5: 252, 1966.

34. Pell, E. M., "Ion Drift in a n-p Junction," *J. Appl. Phys.,* 31: 291-302, 1960.

35. Pell, E. M., "Effect of Li-B Ion Pairing on Li + Ion Drift in Si," *J. Appl. Phys.* 31: 1675-1679, 1960.

36. Pell, E. M., and Ham, F. S., "Recombination Kinetics for Thermally Disassociated Li-B Ion Pair in Si," *J. Appl. Phys.* 32: 1052-1063, 1961.

37. Maita, J. P., "Ion Pairing in Silicon," *J. Phys. Chem. Solids,* 4: 68-70, 1958.

38. Spitzer, W. G., and Waldner, M., "Localized Mode Measurements of Boron and Lithium-Doped Silicon," *J. Appl. Phys.* 36(8): 2450-2453, 1965.

39. Corbett, J. W., Watkins, G. D., and McDonald, R. S., "New Oxygen Infrared Bands in Annealed Irradiated Silicon," *Phys. Rev.* 135: (A1381-1385), 1964.

40. Whan, R. E., "Oxygen-Defect Complexes in Neutron-Irradiated Silicon," *J. Appl. Phys.* 37: 3378-3382, 1966.

41. Corelli, J. C., Oehler, G., Becker, J. F., and Eisentraut, J. K., "Annealing of Infrared Defect Absorption Bands in 40-Me-V Electron-Irradiated Silicon," *J. Appl. Phys.* 36: 1787-1788, 1965.

42. Fan, H. Y., and Ramdas, A. K., "Infrared Absorption and Photoconductivity in Irradiated Silicon," *J. Appl. Phys.* 30: 1127-1134, 1959.

43. Vavilov, V. S., and Plotnikov, A. F., "Defects Introduced into Silicon by Fast Electron and Neutron Irradiation," *J. Phys. Soc. Japan,* 18, Suppl III: 230-236, 1963.

44. Almelch, N., and Goldstein, Bernard, "Electron Paramagnetic Resonance and Electrical Properties of the Dominant Paramagnetic Defect in Electron-Irradiated p-Type Silicon," *Phys. Review,* 149: 687-692, 1966.

45. Bemski, G., and Dias, C. A., "Quenched in Defects in p-Type Silicon," *J. Appl. Phys.* 35: 2983-2985, 1964.

46. Swalin, R. A., *J. Phys. Chem. Solids,* 18: 290, 1961.

47. Benneman, K. H., "New Method for Testing Lattice Point Defects in Covalent Crystals," *Phys. Rev.* 137: (A1497-A1514), 1965.

48. Nakano, T., Nakasima, K., and Inuishi, Y., "Radiation Damage of Carrier Life Time in P Type Si," *J. Phys. Soc. Japan* 20(12): 2140-2146, December 1965.

"The aeronautical and space activities of the United States shall be conducted so as to contribute . . . to the expansion of human knowledge of phenomena in the atmosphere and space. The Administration shall provide for the widest practicable and appropriate dissemination of information concerning its activities and the results thereof."

—NATIONAL AERONAUTICS AND SPACE ACT OF 1958

NASA SCIENTIFIC AND TECHNICAL PUBLICATIONS

TECHNICAL REPORTS: Scientific and technical information considered important, complete, and a lasting contribution to existing knowledge.

TECHNICAL NOTES: Information less broad in scope but nevertheless of importance as a contribution to existing knowledge.

TECHNICAL MEMORANDUMS: Information receiving limited distribution because of preliminary data, security classification, or other reasons.

CONTRACTOR REPORTS: Scientific and technical information generated under a NASA contract or grant and considered an important contribution to existing knowledge.

TECHNICAL TRANSLATIONS: Information published in a foreign language considered to merit NASA distribution in English.

SPECIAL PUBLICATIONS: Information derived from or of value to NASA activities. Publications include conference proceedings, monographs, data compilations, handbooks, sourcebooks, and special bibliographies.

TECHNOLOGY UTILIZATION PUBLICATIONS: Information on technology used by NASA that may be of particular interest in commercial and other non-aerospace applications. Publications include Tech Briefs, Technology Utilization Reports and Notes, and Technology Surveys.

Details on the availability of these publications may be obtained from:

SCIENTIFIC AND TECHNICAL INFORMATION DIVISION

NATIONAL AERONAUTICS AND SPACE ADMINISTRATION

Washington, D.C. 20546